Available online at www.sciencedirect.com
SCIENCE DIRECT
Tetrahedron
ELSEVIER
Tetrahedron 62 (2006) 6073–6081

Longipedlactones A–I, nine novel triterpene dilactones possessing a unique skeleton from *Kadsura longipedunculata*

Jian-Xin Pu,[a] Rong-Tao Li,[a] Wei-Lie Xiao,[a] Ning-Bo Gong,[b] Sheng-Xiong Huang,[a] Yang Lu,[b] Qi-Tai Zheng,[b] Li-Guang Lou[c] and Han-Dong Sun[a,*]

[a]*State Key Laboratory of Phytochemistry and Plant Resources in West China, Kunming Institute of Botany, Chinese Academy of Sciences, Kunming 650204, Yunnan, PR China*
[b]*Institute of Materia Medica, Chinese Academy of Medical Sciences and Peking union Medical College, Peking 100050, PR China*
[c]*Shanghai Institute of Materia Medica, Shanghai Institutes for Biological Science, Chinese Academy of Sciences, Shanghai 200032, PR China*

Received 5 February 2006; revised 29 March 2006; accepted 31 March 2006
Available online 2 May 2006

Abstract—Nine novel triterpene dilactones with an unprecedented rearranged pentacyclic skeleton, longipedlactones A–I (**1**–**9**), have been isolated from the leaves and stems of *Kadsura longipedunculata* Finet et Gagnep (Schisandraceae). Their structures were determined on the basis of comprehensive spectroscopic analysis and single-crystal X-ray structure determination. A biogenetic pathway for longipedlactone A (**1**) was also proposed. Compounds **1**–**3**, **6**, and **8** showed significant cytotoxicity against A549, with HT-29 and K562 cell lines having IC_{50} values of 0.84–11.38 μM in vitro.
© 2006 Elsevier Ltd. All rights reserved.

1. Introduction

The genus *Kadsura* belongs to the family Schisandraceae. Some species of this genus have been reported to contain dibenzocyclooctadienlignans, lanostane, and cycloartane triterpenoids, including anti-HIV, antitumor, anti-HBeAg, and anti-lipid peroxidative activities.[1–8] Nowadays, some novel triterpenoids and lignans with unprecedented new skeletons, such as kadsuphilactone A and taiwankadsurins A–C,[9,10] have been isolated from this genus. Therefore, in the research field of phytochemistry, this genus is of interest for the identification of new natural compounds with interesting biological activities, and the investigation of natural compounds that have potential as natural sources of intermediates for the synthesis of high-added-value compounds.

Kadsura longipedunculata Finet et Gagnep is a climbing plant widely distributed in the southern part of China. It has been used in folk medicine for the treatment of rheumatoid arthritis as well as gastric and duodenal ulcers.[11,12] Previously, we reported the isolation and structure elucidations of two novel triterpenoids, kadlongilactones A and B. These have a unique skeleton and are extracted from the leaves and stems of *K. longipedunculata*.[13] In the continuous search for bioactive metabolites from this plant, nine novel triterpene derivatives, longipedlactones A–I (**1**–**9**), were isolated, which featured an unprecedented rearranged pentacyclic backbone derived from cycloartane. The C and D rings of longipedlactones A–I were rearranged to 5/6 consecutive carbocycle systems with an exocyclic double bond in the D ring, which is different from the previously isolated 6/5 consecutive carbocycles of lancilactones A and B.[3] In this paper, the isolation, structure elucidation, and plausible hypotheses on the biogenetic pathway are described. The biological activity of these novel compounds is also reported.

2. Results and discussion

Longipedlactone A (**1**) was isolated as colorless crystals, which gave a $[M-H]^-$ ion at *m*/*z* 477.2630 in HR-ESIMS consistent with a molecular formula $C_{30}H_{38}O_5$ (calcd 477.2640 for $C_{30}H_{37}O_5$), requiring 12 sites of unsaturation. The UV spectrum of **1** showed absorption maxima at 224, 254 and 280 nm, indicating the presence of conjugated systems. The IR spectrum showed the presence of hydroxyl group (3464 cm^{-1}) and two lactone groups (1655 and 1695 cm^{-1}). The ^1H NMR spectrum (Table 1) exhibited signals for one secondary methyl (δ_H 1.14, d, J=7.3 Hz), four tertiary methyls (δ_H 1.03, 1.48, 1.53, and 1.86), five olefinic proton signals (δ_H 5.70, 5.74, 6.25, 6.66, and 6.72), and

Keywords: Longipedlactones A–I; *Kadsura longipedunculata*; Structure elucidation; Biogenesis; Bioactivity.
* Corresponding author. Tel.: +86 871 5223251; fax: +86 871 5216343; e-mail: hdsun@mail.kib.ac.cn

0040–4020/$ - see front matter © 2006 Elsevier Ltd. All rights reserved.
doi:10.1016/j.tet.2006.03.108

Table 1. ^{1}H NMR spectroscopic data of compounds **1–5**[a]

Proton	1	2	3	4	5
1	6.66 (d, 12.2)	6.70 (d, 12.4)	6.61 (d, 12.3)	5.89 (dd, 1.5, 12.5)	6.50 (d, 12.4)
2	5.70 (d, 12.2)	5.72 (d, 12.4)	6.04 (d, 12.3)	6.34 (d, 12.5)	5.90 (d, 12.4)
5	3.75 (br d, 9.8)	3.79 (br d, 9.4)	4.10 (br d, 9.3)	2.92 (overlap)	4.02 (br d, 9.4)
6α	2.13 (overlap)	2.06 (overlap)	2.16 (overlap)	2.02–2.10 (m)	2.10 (overlap)
6β	1.15 (overlap)	1.69 (overlap)	1.69 (overlap)	1.24–1.30 (m)	1.03–1.14 (m)
7α	2.00 (overlap)	2.13 (overlap)	2.22–2.25 (m)	1.91 (overlap)	2.19–2.26 (m)
7β	1.73–1.75 (m)	1.70 (overlap)	1.32 (overlap)	1.54–1.57 (m)	1.64–1.69 (m)
8	1.39 (dd, 2.6, 12.4)	1.64 (overlap)	1.66 (overlap)	1.64 (overlap)	1.55 (dd, 1.7, 12.2)
11α	2.16 (overlap)	1.95 (overlap)	2.14 (overlap)	2.53 (dd, 8.0, 13.1)	2.45 (dd, 8.1, 13.3)
11β	1.65 (overlap)	1.78–1.84 (m)	1.86 (overlap)	2.14 (overlap)	2.14 (overlap)
12	2.78 (dd, 8.5, 10.7)	2.57 (dd, 7.0, 13.0)	3.12 (dd, 6.8, 13.3)	3.08 (t, 8.6)	3.10 (dd, 8.1, 10.7)
15α	1.60 (overlap)	0.99 (overlap)	1.44 (overlap)	1.81 (dd, 3.0, 16.4)	1.71 (overlap)
15β	2.05 (overlap)	1.28–1.33 (m)		2.17 (overlap)	2.07 (overlap)
16α	5.74 (d, 2.6)	1.51 (overlap)	2.08 (overlap)	5.85 (overlap)	5.97 (d, 3.0)
16β		1.63 (overlap)	1.84 (overlap)		
17		2.15 (overlap)			
18a	4.96 (br s)	4.94 (d, 2.2)	5.58 (d, 2.3)	5.07 (br s)	5.25 (br s)
18b	4.84 (br s)	4.73 (d, 2.2)	5.27 (d, 2.3)	4.90 (br s)	4.96 (br s)
19	6.25 (s)	6.31 (s)	6.26 (s)	3.42 (s)	6.41 (s)
20	2.89–2.92 (m)	2.01 (overlap)	2.29–2.31 (m)	2.95 (overlap)	3.30–3.35 (m)
21	1.14 (d, 7.3)	0.96 (d, 7.2)	1.27 (d, 6.8)	1.12 (d, 7.0)	1.31 (d, 7.3)
22	4.44 (ddd, 4.3, 6.0, 11.1)	4.63 (ddd, 4.4, 8.3, 13.2)	5.09–5.13 (m)	4.49 (ddd, 5.0, 6.8, 11.6)	4.77 (dd, 4.1, 7.5)
23α	2.27 (overlap)	2.24 (overlap)	2.79–2.84 (m)	2.20 (overlap)	4.70 (br s)
23β	2.36 (overlap)	2.34–2.42 (m)	2.49–2.57 (m)	2.15 (overlap)	
24	6.72 (br d, 5.2)	6.75 (dd, 1.7, 6.6)	6.51 (br d, 6.3)	6.45 (br d, 6.1)	6.75 (d, 1.3)
27	1.86 (s)	1.86 (s)	1.95 (s)	1.86 (s)	1.90 (s)
28	1.03 (s)	0.92 (s)	1.12 (s)	1.21 (s)	1.27 (s)
29	1.48 (s)	1.48 (s)	1.42 (s)	1.36 (s)	1.40 (s)
30	1.53 (s)	1.54 (s)	1.46 (s)	1.62 (s)	1.42 (s)
9-OH	4.56 (s)		6.57 (s)	6.50 (s)	6.48 (s)
17-OH			5.96 (s)		
23-OH					7.42 (d, 5.6)

[a] Data were recorded on a Bruker DRX-500 MHz spectrometer, chemical shift values δ are in ppm, and the coupling constant J is in Hz (in parentheses). Data of compounds **1** and **2** were recorded in CD_3OD, and compounds **3**, **4**, and **5** were recorded in C_5D_5N.

a characteristic exocyclic methylene (δ_H 4.84 and 4.96, each br s). Analysis of ^{13}C NMR, DEPT, and HSQC data revealed that **1** contains two α,β-unsaturated carbonyl carbons, seven quaternary carbons (including four olefinic and one oxygenated carbons), 10 methines (including five olefinic and one oxygenated), six methylenes (including an exocyclic methylene), and five methyls (including one secondary methyl). Apart from five double bonds and two carbonyl groups, the remaining elements of unsaturation in **1** were assumed to be a pentacyclic skeleton. These data were consistent with the HRMS empirical formula and suggested that **1** was probably a pentacyclic triterpene. Since the NMR data of **1** were quite distinctive from those of the known triterpene skeleton, the possible structure of **1** was firstly established by a detailed analysis of 2D-NMR data, and finally confirmed by single-crystal X-ray analysis.

Extensive analysis of ^{1}H–^{1}H COSY, HMBC, and HSQC spectral data led to the establishment of three substructures **1a**–**1c** (Fig. 1), which were deduced as follows. In the HMBC spectrum (Fig. 2), the correlations of CH_3-30 (δ_H 1.53, s) with C-4, C-5, and C-29, and of CH_3-29 (δ_H 1.48, s) with C-4 and C-30, required that CH_3-30 and CH_3-29 be attached to the same oxygenated quaternary carbon (δ_C 82.5, s, C-4). In addition, the proton signal at δ_H 5.70 (d, J=12.2 Hz, H-2) showed HMBC correlations with C-3 and C-10, and the proton signal at δ_H 3.75 (br d, J=9.8 Hz, H-5) showed correlations with C-1, C-4, C-19, and C-29. Other correlations were noted between H-19 (δ_H 6.25, s) and C-8, C-9. These facts, along with two proton spin systems (**a** and **b**) deduced from ^{1}H–^{1}H COSY correlations (Fig. 2), and the lack of any absorption band due to carboxylic group in the IR spectrum, led to the establishment of substructure **1a**. HMBC correlations were observed from CH_3-28 (δ_H 1.03, s) to C-12, C-14, and C-15, from H_2-18 (δ_H 4.96-a, 4.84-b, each br s) to C-12, C-13, and C-17, and from CH_3-21 (δ_H 1.14, d, J=7.3 Hz) to C-17 and C-20. The above evidence, in combination with two proton spin systems (**c** and **d**), determined the existence of substructure **1b**. Furthermore, HMBC correlations from CH_3-27 (δ_H 1.86, s) to C-24, C-25, and C-26, together with the critical MS

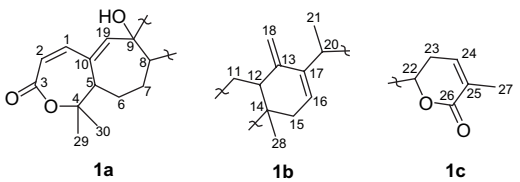

Figure 1. Substructures (**1a**–**1c**) of **1**.

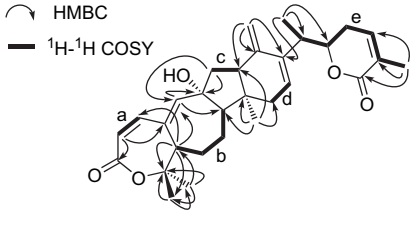

Figure 2. Key ^{1}H–^{1}H COSY and HMBC correlations of **1**.

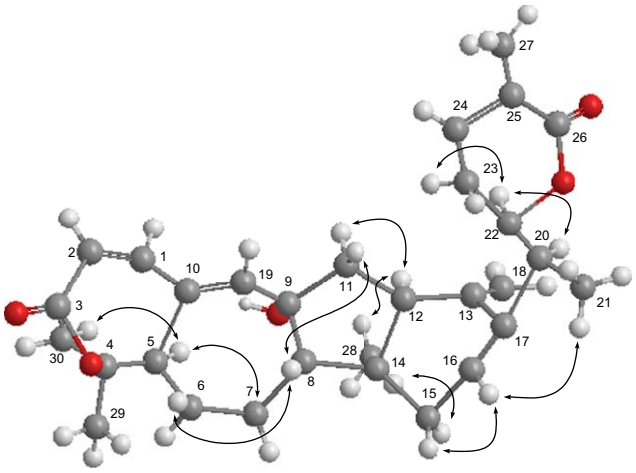

Figure 3. Key ROESY correlations and relative configurations assigned for **1**.

fragment at *m/z* 111 $[C_6H_7O_2]^-$, indicated the presence of a six-membered α-methyl-α,β-unsaturated lactone ring (**1c**).[3] In the HMBC spectrum, the proton signal H-11β (δ_H 1.65, overlap) showed correlations with C-9 and C-19, and CH_3-28 showed correlation with C-8 requiring the connection of **1a** and **1b**. In addition, HMBC correlation from CH_3-21 to C-22, in conjunction with proton spin system (**e**) (Fig. 2), determined the direct combination of **1b** and **1c**. Accordingly, the planar structure of **1** could be established. Its relative stereochemistry was determined by ROESY (Fig. 3) experiment and X-ray crystallographic analysis (Fig. 4). Thus, the structure of **1** was established as shown in Scheme 1.

Longipedlactone B (**2**) was obtained as an amorphous powder. Its molecular formula, $C_{30}H_{40}O_5$, was determined by the $[M-1]^-$ ion peak in the negative HR-ESIMS at *m/z* 479.2794 (calcd 479.2797). The ^1H and ^{13}C NMR spectra of **2** showed close resemblance to that of **1**, the obvious differences were the absence of a double bond between C-16 and C-17 (δ_C 126.7, d and 141.7, s) in **1**, and the presence of a methylene (δ_C 25.9, t) and a methine (δ_C 44.5, d) in **2**, which indicated that a double bond in **1** was reduced. HMBC and ^1H–^1H COSY spectra confirmed the above deduction. On the basis of these observations, the structure of **2** was proposed as shown in Scheme 1 and its relative stereochemistry was determined to be the same as that of **1** by the analysis of ROESY data.

Longipedlactone C (**3**) was obtained as an amorphous powder with the empirical formula $C_{30}H_{40}O_6$, in agreement with the HR-ESIMS (*m/z* 495.2748 $[M-1]^-$, calcd for $C_{30}H_{39}O_6$, 495.2746) and ^{13}C NMR spectral data. The NMR data of **3** were strikingly similar to those of **2**, except for the lack of a methine at δ_C 44.5 (C-17), the appearance of a new oxygenated quaternary carbon (δ_C 75.3, s) and a hydroxyl group (δ_H 5.96, s) in **3**. HMBC (Fig. 5) correlations observed from the proton signal of OH to C-13, C-17, and C-20 indicated this hydroxyl group to be located at C-17. In the ROESY (Fig. 5) spectrum, OH-17 had ROE correlations with H-16β and H-21β, indicating OH-17 to be in β-orientation. Thus, the structure of **3** was determined to be 17β-hydroxyl-longipedlactone B.

HR-ESIMS analysis of longipedlactone D (**4**) demonstrated that it has the molecular formula $C_{30}H_{38}O_6$, differing from **1** by the addition of an oxygen atom. Detailed comparison of ^1H and ^{13}C NMR data of **4** with those of **1** was analogous. The only significant differences include the appearance of a trisubstituted epoxide (δ_C 62.4, s and 67.1, d; δ_H 3.42, s) in **4** and the disappearance of a double bond (δ_C 146.5 and 149.1; δ_H 6.25, s) in **1**. The HMBC (Fig. 5) correlations of H-2 and H-5 with C-10, of H-1 with C-19, and of H-19 with C-9, C-10, and C-11 verified that the epoxide group was positioned between C-10 and C-19. This assignment was in accord with the observed downfield chemical shifts for the C-1 and C-2 signals from δ_C 146.8 and 118.5 in **1** to δ_C 145.1 and 126.1 in **4**, respectively. In the ROESY (Fig. 5) experiment, H-19 showed correlations with H-1, H-8β, and H-11β, indicating an α-orientation of the epoxy ring.

HR-ESIMS of longipedlactone E (**5**) gave a quasi-molecular ion at *m/z* 517.2558 $[M+Na]^+$, corresponding to the molecular formula $C_{30}H_{38}O_6$, indicating 16 mass units more than compound **1**. The signals in its ^1H and ^{13}C NMR

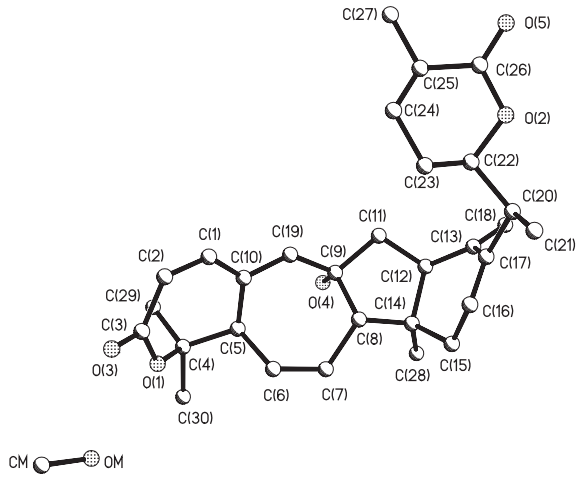

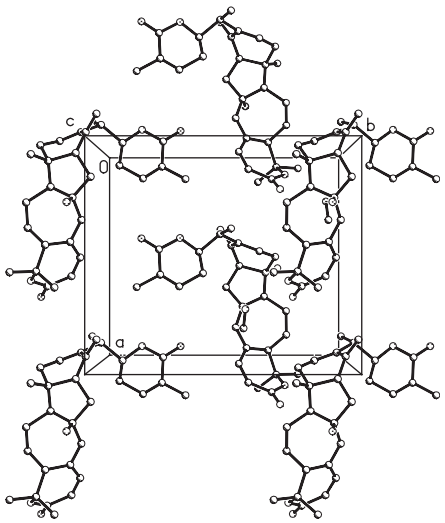

Figure 4. X-ray crystal structure of **1**.

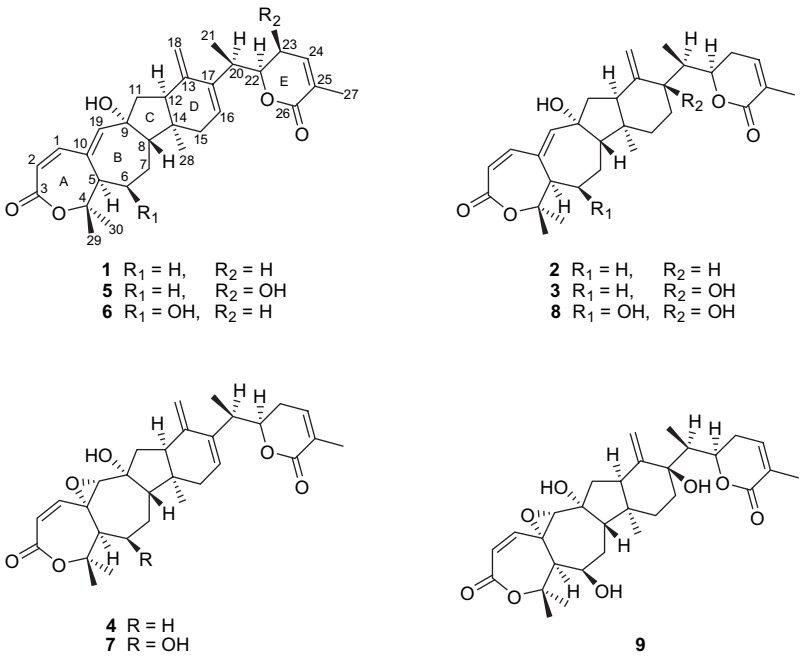

1 R_1 = H, R_2 = H
5 R_1 = H, R_2 = OH
6 R_1 = OH, R_2 = H

2 R_1 = H, R_2 = H
3 R_1 = H, R_2 = OH
8 R_1 = OH, R_2 = OH

4 R = H
7 R = OH

9

Scheme 1. Structures of longipedlactones A–I (**1**–**9**).

spectra strikingly matched those of **1** (Tables 1 and 3). The only significant differences included the obvious presence of a new hydroxyl group (δ_H 7.42, d, J=5.6 Hz), and the lack of a H_2-23 signal in the ^{1}H NMR spectrum, implying that this new hydroxyl group is present at C-23. This was further confirmed by the HMBC (Fig. 5) correlations of H-22 and H-20 with C-23 (δ_C 63.3, d). The ROESY (Fig. 5) experiment of **5** showed correlations between H-23/H-20α, H-23/H-11β, and H-22α/H-20α. This, along with the smaller value of cis-coupling constants of H-22 in the ^{1}H NMR spectrum, confirmed OH-23 to be in β-orientation.

Longipedlactone F (**6**) was obtained as colorless crystals. Its molecular formula $C_{30}H_{38}O_6$ was determined by the $[M+Na]^+$ ion peak at m/z 517.2576 (calcd for $C_{30}H_{38}O_6Na$,

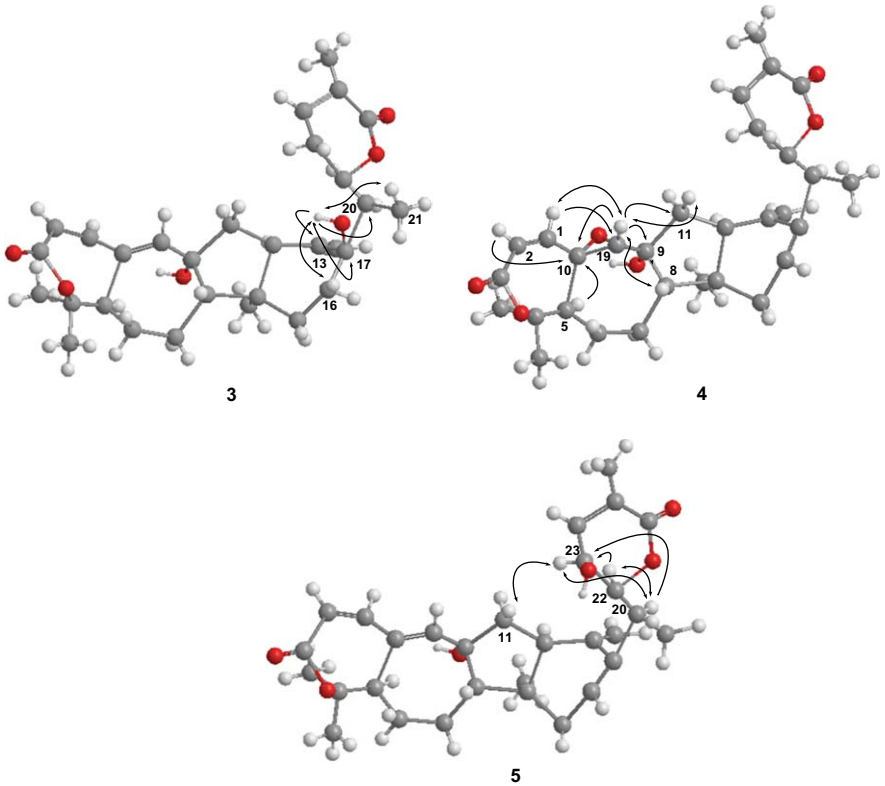

3 **4** **5**

Figure 5. Key HMBC (→) and ROESY (↔) correlations and relative configurations assigned for **3**–**5**.

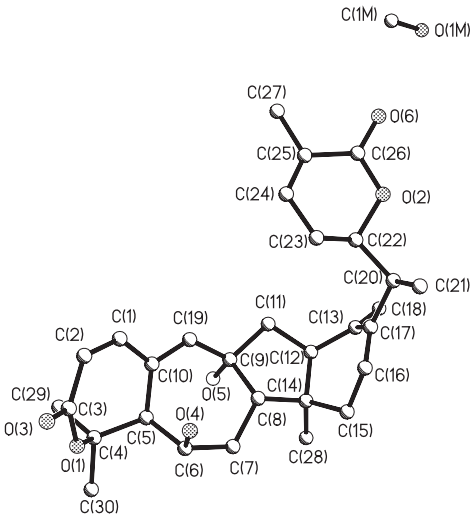

Figure 6. X-ray crystal structure of **6** showing relative configuration.

517.2566) in the HR-ESIMS. The NMR spectra of **6** were quite similar to those of **1**, suggesting that they had the same basic structure with the difference as observed between **2** and **3**. Thus, **6** was considered to have a new hydroxyl group located at C-6 (δ_C 65.4, d), which was confirmed by the HMBC correlations observed from H-19, H-5 and H-8 to C-6. Furthermore, **6** was obtained as colorless crystals after several recrystallizations in methanol solvent. The analysis of the single-crystal X-ray diffraction (Fig. 6) confirmed the relative configuration of **6** as proposed in Scheme 1, which showed a β-orientation for OH-6.

Longipedlactone G (**7**) was obtained as an amorphous powder. The $[M-H]^-$ ion peak at *m/z* 509.2550 (calcd for $C_{30}H_{37}O_7$, 509.2539) in the HR-ESIMS determined its molecular formula to be $C_{30}H_{38}O_7$. Side-by-side comparison of the ^1H and ^{13}C NMR data (Tables 2 and 3) between **7** and **6** indicated that these two compounds were almost identical, except for the presence of a trisubstituted epoxide (δ_C 60.8, s and 68.1, d; δ_H 3.39, s) in **7** and the disappearance of a double bond (δ_C 141.9 and 147.1; δ_H 6.60, s) in **6**. The epoxide group was positioned between C-10 and C-19 on the basis of HMBC correlations, which was same as that observed in **4**. The ROESY spectrum indicated the epoxide group was in an α-orientation similar to that of **4**. Thus, **7** had the structure shown in Scheme 1.

The structures of longipedlactones H (**8**) and I (**9**) were determined to be as shown in Scheme 1 on the basis of spectral data comparisons in an analogous manner to the structure elucidation of **3**, **4**, and **6**. The locations of hydroxyl group and epoxide group were assigned by the observed HMBC and ^1H–^1H COSY (Figs. 7 and 8) correlations. ROESY correlations observed between H-6/H-5α, H-6/H-7α and OH-17/H-16β, OH-17/H-18a were consistent with a β-orientation of OH-6 and OH-17 in **8** and **9**, respectively. Furthermore, ROEs between H-19/H-1, H-19/H-8β, and H-19/H-11β indicated that the epoxy ring of **9** was in an α-orientation like that of **4** and **7**. Therefore, the structures of **8** and **9** were determined to be 6β-hydroxy-longipedlactone C and 9,19α-epoxy-longipedlactone H, and were named as longipedlactones H and I, respectively.

Table 2. ^1H NMR spectroscopic data of compounds **6–9**[a]

Proton	6	7	8	9
1	6.80 (d, 12.2)	5.91 (d, 12.2)	6.84 (d, 12.4)	5.95 (dd, 1.5, 12.5)
2	6.00 (d, 12.2)	6.35 (d, 12.2)	6.05 (d, 12.4)	6.42 (d, 12.5)
5	4.37 (br s)	3.03 (overlap)	4.40 (br s)	3.07 (br s)
6α	4.89 (br s)	4.80 (d, 4.4)	4.89 (br s)	4.85 (br s)
7α	2.43–2.46 (m)	2.07 (overlap)	2.47 (overlap)	2.14–2.20 (m)
7β	2.06 (overlap)	1.86 (overlap)	2.02 (overlap)	1.92–1.96 (m)
8	2.32–2.36 (m)	2.56 (d, 11.3)	2.56 (overlap)	2.75 (overlap)
11α	2.51–2.54 (m)	2.61 (dd, 7.9, 13.5)	2.19 (overlap)	2.24 (dd, 7.0, 12.5)
11β	1.81 (overlap)	2.18 (overlap)	1.93 (overlap)	2.03 (overlap)
12	3.12 (t, 8.8)	3.05 (overlap)	3.13 (dd, 6.0, 12.9)	3.19 (dd, 7.0, 13.6)
15α	1.67 (d, 15.6)	1.87 (overlap)	1.40–1.41 (m)	1.54–1.62 (m)
15β	2.16 (overlap)	2.22 (overlap)		1.46–1.50 (m)
16α	5.61 (d, 4.0)	5.71 (br s)	1.89 (overlap)	2.07–2.10 (m)
16β			1.65–1.68 (m)	1.72–1.75 (m)
18a	5.09 (br s)	5.19 (br s)	5.56 (d, 2.0)	5.58 (d, 2.6)
18b	4.94 (br s)	4.97 (br s)	5.29 (d, 2.0)	5.30 (d, 2.6)
19	6.60 (s)	3.39 (s)	6.50 (overlap)	3.37 (s)
20	3.05 (t, 12.3)	3.08–3.10 (m)	2.21 (overlap)	2.31–2.33 (m)
21	1.07 (d, 7.0)	1.09 (d, 6.9)	1.26 (d, 6.9)	1.23 (d, 7.0)
22	4.47 (ddd, 4.0, 9.1, 10.1)	4.47 (ddd, 4.4, 9.3, 12.2)	4.82–4.84 (m)	4.95 (overlap)
23α	2.01 (overlap)	2.21 (overlap)	2.75–2.79 (m)	2.78 (overlap)
23β	2.11 (overlap)	2.11 (overlap)	2.52 (overlap)	2.46–2.53 (m)
24	6.48 (dd, 1.8, 4.0)	6.51 (br d, 5.9)	6.50 (overlap)	6.48 (br d, 6.7)
27	1.85 (s)	1.87 (s)	2.01 (s)	1.98 (s)
28	1.30 (s)	1.23 (s)	1.15 (s)	1.11 (s)
29	1.50 (s)	1.43 (s)	1.50 (s)	1.44 (s)
30	1.52 (s)	1.74 (s)	1.54 (s)	1.77 (s)
6-OH	6.31 (s)	6.68 (d, 4.4)		
9-OH	6.56 (s)	6.41 (s)	6.57 (s)	6.36 (s)
17-OH			5.86 (s)	5.87 (s)

[a] Data were recorded on a Bruker DRX-500 MHz spectrometer, chemical shift values δ are in ppm, and the coupling constant *J* is in Hz (in parentheses). Data of compounds **6–9** were recorded in C_5D_5N.

Table 3. ^{13}C NMR spectroscopic data of compounds **1–9**[a]

Carbon	1	2	3	4	5	6	7	8	9
1	146.8 (d)	146.6 (d)	144.2 (d)	145.1 (d)	144.2 (d)	146.3 (d)	146.6 (d)	146.3 (d)	146.7 (d)
2	118.5 (d)	118.6 (d)	119.3 (d)	126.1 (d)	119.1 (d)	119.7 (d)	126.7 (d)	120.0 (d)	126.8 (d)
3	169.5 (s)	169.5 (s)	166.6 (s)	165.6 (s)	166.5 (s)	166.9 (s)	166.6 (s)	166.7 (s)	166.6 (s)
4	82.5 (s)	82.4 (s)	80.3 (s)	81.5 (s)	79.8 (s)	80.0 (s)	81.1 (s)	80.0 (s)	81.0 (s)
5	49.5 (d)	49.4 (d)	48.7 (d)	49.7 (d)	48.8 (d)	52.8 (d)	53.3 (d)	53.1 (d)	53.5 (d)
6	29.5 (t)	28.7 (t)	28.1 (t)	26.4 (t)	28.3 (t)	65.4 (d)	65.8 (d)	65.9 (d)	66.1 (d)
7	28.2 (t)	29.4 (t)	28.6 (t)	24.9 (t)	27.5 (t)	36.3 (t)	34.4 (t)	36.9 (t)	34.9 (t)
8	57.4 (d)	55.0 (d)	54.5 (d)	56.3 (d)	56.2 (d)	49.3 (d)	47.4 (d)	46.9 (d)	47.3 (d)
9	80.8 (s)	80.9 (s)	79.7 (s)	77.9 (s)	79.8 (s)	79.5 (s)	77.6 (s)	79.8 (s)	78.3 (s)
10	146.5 (s)	146.9 (s)	145.8 (s)	62.4 (s)	144.6 (s)	141.9 (s)	60.8 (s)	142.1 (s)	61.0 (s)
11	51.7 (t)	48.5 (t)	48.3 (t)	51.0 (t)	51.0 (t)	51.7 (t)	51.1 (t)	48.5 (t)	48.2 (t)
12	54.1 (d)	54.5 (d)	53.7 (d)	53.5 (d)	53.5 (d)	53.4 (d)	52.9 (d)	53.9 (d)	54.8 (d)
13	149.7 (s)	149.2 (s)	153.4 (s)	148.5 (s)	148.6 (s)	148.3 (s)	147.6 (s)	153.5 (s)	153.3 (s)
14	44.9 (s)	45.1 (s)	44.9 (s)	43.4 (s)	44.2 (s)	43.7 (s)	42.3 (s)	44.3 (s)	43.4 (s)
15	38.1 (t)	36.0 (t)	34.2 (t)	37.3 (t)	37.5 (t)	37.2 (t)	36.8 (t)	33.7 (t)	34.6 (t)
16	126.7 (d)	25.9 (t)	35.1 (t)	125.4 (d)	127.0 (d)	126.2 (d)	125.7 (d)	35.1 (t)	35.6 (t)
17	141.7 (s)	44.5 (d)	75.3 (s)	140.2 (s)	140.4 (s)	139.8 (s)	138.7 (s)	75.3 (s)	75.3 (s)
18	108.2 (t)	115.6 (t)	115.6 (t)	108.2 (t)	108.1 (t)	108.2 (t)	109.3 (t)	115.9 (t)	115.5 (t)
19	149.1 (d)	148.5 (d)	147.3 (d)	67.1 (d)	148.0 (d)	147.1 (d)	68.1 (d)	146.5 (d)	66.7 (d)
20	41.1 (d)	42.2 (d)	44.3 (d)	40.1 (d)	38.6 (d)	39.8 (d)	38.9 (d)	45.3 (d)	43.4 (d)
21	15.8 (q)	13.7 (q)	9.5 (q)	16.3 (q)	16.6 (q)	14.0 (q)	14.5 (q)	9.4 (q)	9.5 (q)
22	82.5 (d)	81.2 (d)	79.7 (d)	81.1 (d)	86.2 (d)	80.2 (d)	80.3 (d)	79.6 (d)	79.5 (d)
23	27.5 (t)	24.7 (t)	27.1 (t)	27.1 (t)	63.3 (d)	25.7 (t)	25.8 (t)	27.1 (t)	27.1 (t)
24	141.6 (d)	142.1 (d)	141.4 (d)	139.7 (d)	144.6 (d)	139.9 (d)	140.4 (d)	141.3 (d)	141.3 (d)
25	128.9 (s)	128.7 (s)	127.6 (s)	128.1 (s)	127.4 (s)	128.1 (s)	127.7 (s)	127.8 (s)	127.7 (s)
26	168.2 (s)	168.6 (s)	166.6 (s)	166.0 (s)	164.8 (s)	166.0 (s)	166.1 (s)	166.9 (s)	166.5 (s)
27	16.9 (q)	16.9 (q)	17.1 (q)	17.1 (q)	17.0 (q)	17.1 (q)	17.1 (q)	17.2 (q)	17.1 (q)
28	27.4 (q)	26.3 (q)	25.9 (q)	27.0 (q)	27.5 (q)	27.5 (q)	26.1 (q)	26.3 (q)	25.8 (q)
29	29.3 (q)	29.5 (q)	29.4 (q)	29.2 (q)	29.4 (q)	30.0 (q)	30.0 (q)	30.0 (q)	29.9 (q)
30	26.0 (q)	25.9 (q)	25.9 (q)	25.0 (q)	26.3 (q)	26.7 (q)	26.2 (q)	26.8 (q)	26.0 (q)

[a] Data were recorded on a Bruker DRX-500 MHz spectrometer, chemical shift values δ are in ppm, assignments were confirmed by ^{1}H–^{1}H COSY, HSQC, and HMBC.

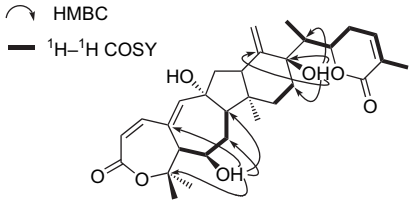

Figure 7. Key ^{1}H–^{1}H COSY and HMBC correlations of **8**.

The cytotoxicity of compounds **1–4** and **6–8** was tested against A549, HT-29 and K562 cell lines in vitro. Compounds **1–3**, **6**, and **8** showed promising cytotoxicity against all three cell lines at the level of IC_{50} values of 0.84–11.38 μM, and no cytotoxicity was observed for compounds **4** and **7** (Table 4). Comparing the structures of these compounds, it was noticeable that the formation of a double bond between C-10 and C-19 conjugated with an α,β-unsaturated lactone in **1–3**, **6**, and **8** made them have a significant IC_{50} values. In contrast, for **4** and **7**, the epoxy ring is displaced by the double bond, which destroys the conjugated system, resulting in no cytotoxicity. From the above observation, it was reasonable to presume that the big conjugated system (α,β,γ,δ-unsaturated lactone) was probably of crucial importance in its antitumor activity. Further investigation on the bioactivity of this series of triterpenoids will be of emphasis in our future research. Due to the small quantity of compounds **5** and **9**, their cytotoxicity was not determined.

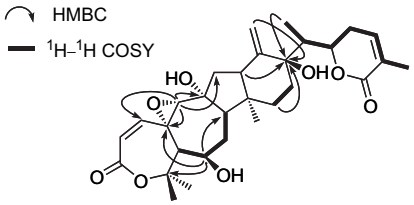

Figure 8. Key ^{1}H–^{1}H COSY and HMBC correlations of **9**.

A plausible biogenetic pathway for longipedlactone A (**1**) was proposed on the basis of kadsudilactone[14] isolated from the same plant, *K. longipedunculata*, Scheme 2. After ring expansion, oxidation and dehydrogenation of kadsudilactone result in intermediate **A**, this is followed by hydroxylation on C-13 to afford intermediate **B**, which then undergoes a Wagner–Meerwein rearrangement and hydroxylation at C-9 (**c–e**) to give **E**.[15] Finally, hydroxylation at C-17 and dehydration at C-16 and C-17 yielded longilactone A (**1**).

Table 4. Cytotoxic activities of compounds **1–4** and **6–8** against tumor cell lines

Compd	IC_{50} (μM)		
	A 549	HT-29	K562
1	1.82	1.64	2.96
2	2.47	1.81	2.72
3	0.24	1.01	1.49
4	>100	>100	>100
6	5.56	2.24	3.55
7	>100	>100	>100
8	11.38	5.63	7.58

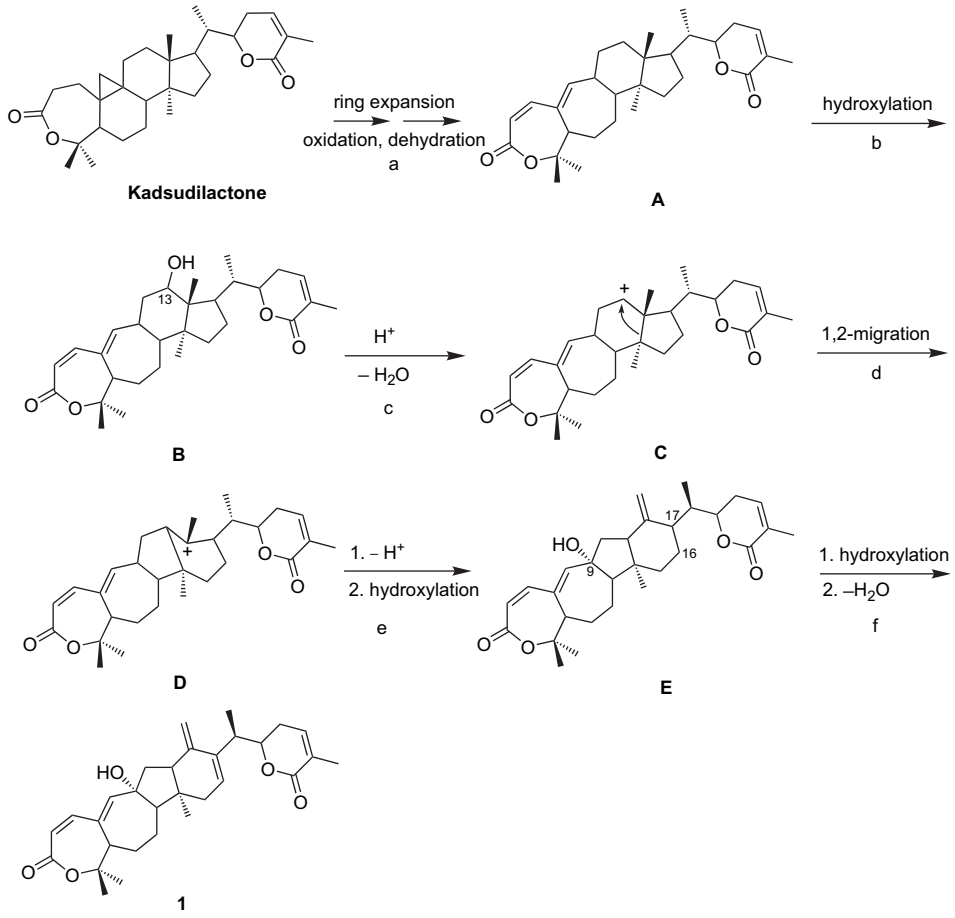

Scheme 2. Plausible biogenetic pathway for longipedlactone A (**1**).

3. Experimental

3.1. General

Melting points were measured on an XRC-1 micro melting point apparatus and were uncorrected. Optical rotations were measured on a JASCO DIP-370 digital polarimeter. IR spectra were obtained on a Bio-Rad FtS-135 spectrophotometer with KBr pellets, whereas UV spectral data were obtained using a UV-210A spectrometer. MS were recorded on a VG Auto Spec-3000 spectrometer. 1D- and 2D-NMR spectra were obtained on the Bruker DRX-500 instruments with TMS as an internal standard.

3.2. Plant material

The leaves and stems of *K. longipedunculata* were collected in Erlang mountain region of Sichuan Province, China, in August 2004, and identified by Prof. Xi-Wen Li, Kunming Institute of Botany. A voucher specimen has been deposited in the Herbarium of the Kunming Institute of Botany, Chinese Academy of Sciences.

3.3. Extraction and isolation

The air-dried and powdered stems and leaves (11 kg) of *K. longipedunculata* were extracted with 70% aqueous Me_2CO (4×30 L) at room temperature to yield an extract, which was successively extracted with petroleum ether and EtOAc. The EtOAc extract (300 g) was subjected to column chromatography over silica gel (1.5 kg, 200–300 mesh) eluting with a $CHCl_3/Me_2CO$ gradient system (9:1, 8:2, 7:3, 6:4, 5:5) to give fractions 1–5. Compounds **1** (40 mg), **2** (8 mg), **3** (16 mg), **4** (4 mg), and **7** (12 mg) were obtained from fraction 1, and compounds **5** (1 mg), **6** (11 mg), **8** (84 mg), and **9** (1 mg) were obtained from fraction 2 after repeated silica gel column chromatographic separations ($CHCl_3$/isopropanol), followed by semipreparative HPLC separation (Agilent 1100 HPLC system, U.S.A; Zorbax SB-C-18, Agilent, 9.4 mm×25 cm, U.S.A., MeOH/H_2O).

3.3.1. Longipedlactone A (1). Colorless crystals; mp 166–167 °C; $[\alpha]_D^{23.9}$ −278.9 (*c* 0.62, C_5H_5N); UV (MeOH): λ_{max} (log ε)=352 (1.20), 280 (4.62), 254 (4.25), 224 nm (4.58); IR (KBr): ν_{max}=3464 (br), 2951, 2924, 2882, 2837, 1710, 1695, 1655, 1131 cm^{-1}; ^1H and ^{13}C NMR data, see Tables 1 and 3; Negative FABMS: *m*/*z* (%): 569 (98) $[M+Gly-H]^-$, 477 (100) $[M-H]^-$, 325 (17), 111 (8); Negative HR-ESIMS: found: 477.2630, calcd 477.2640 for $C_{30}H_{37}O_5$ $[M-H]^-$.

3.3.2. Longipedlactone B (2). White powder; $[\alpha]_D^{24.4}$ −70.5 (*c* 0.42, C_5H_5N); UV (MeOH): λ_{max} (log ε)=279 (4.58), 248 (3.76), 208 nm (4.44); IR (KBr): ν_{max}=3441 (br), 2933, 2867, 1716, 1694, 1126 cm^{-1}; ^1H and ^{13}C NMR data, see Tables 1 and 3; Negative FABMS: *m*/*z* (%): 571 (91)

[M+Gly−H]$^-$, 479 (100) [M−H]$^-$, 325 (23), 139 (25); Negative HR-ESIMS: found: 479.2794, calcd 479.2797 for $C_{30}H_{39}O_5$ [M−H]$^-$.

3.3.3. Longipedlactone C (3). White powder; $[\alpha]_D^{25.6}$ −233.7 (*c* 0.11, C_5H_5N); UV (MeOH): λ_{max} (log ε)=279 nm (4.81); IR (KBr): ν_{max}=3446 (br), 2941, 2867, 1697, 1673, 1129 cm^{-1}; ^{1}H and ^{13}C NMR data, see Tables 1 and 3; Negative FABMS: *m/z* (%): 587 (8) [M+Gly−H]$^-$, 495 (45) [M−H]$^-$, 478 (5) [M−H_2O]$^-$, 139 (100), 111 (5), 99 (25); Negative HR-ESIMS: found: 495.2748, calcd 495.2746 for $C_{30}H_{39}O_6$ [M−H]$^-$.

3.3.4. Longipedlactone D (4). White powder; $[\alpha]_D^{24.6}$ −138.9 (*c* 0.43, C_5H_5N); UV (MeOH): λ_{max} (log ε)=269 (3.17), 225 (4.59), 199 nm (4.37); IR (KBr): ν_{max}=3436 (br), 2980, 2955, 2920, 2879, 2864, 1710, 1692, 1131 cm^{-1}; ^{1}H and ^{13}C NMR data, see Tables 1 and 3; Negative FABMS: *m/z* (%): 585 (31) [M+Gly−H]$^-$, 494 (100) [M]$^-$, 477 (22); Negative HR-ESIMS: found: 493.2576, calcd 493.2590 for $C_{30}H_{37}O_6$ [M−H]$^-$.

3.3.5. Longipedlactone E (5). White powder; $[\alpha]_D^{23.4}$ −206.2 (*c* 0.58, C_5H_5N); UV (MeOH): λ_{max} (log ε)=378 (1.77), 279 (4.87), 229 (4.79), 201 nm (4.86); IR (KBr): ν_{max}=3398 (br), 2955, 2925, 2854, 1718, 1670, 1643, 1130 cm^{-1}; ^{1}H and ^{13}C NMR data, see Tables 1 and 3; Negative FABMS: *m/z* (%): 585 (4) [M+Gly−H]$^-$, 493 (37) [M−H]$^-$, 476 (9), 125 (23), 112 (12), 97 (100); Positive HR-ESIMS: found: 517.2558, calcd 517.2566 for $C_{30}H_{38}O_6Na$ [M+Na]$^+$.

3.3.6. Longipedlactone F (6). Colorless crystals; mp 139–141 °C; $[\alpha]_D^{26.5}$ −283.5 (*c* 0.97, C_5H_5N); UV (MeOH): λ_{max} (log ε)=347 (2.69), 278 (4.56), 225 nm (4.49); IR (KBr): ν_{max}=3613, 3525, 3442, 2982, 2948, 2926, 2834, 1717, 1666, 1636, 1614, 1125 cm^{-1}; ^{1}H and ^{13}C NMR data, see Tables 2 and 3; Negative FABMS: *m/z* (%): 585 (10) [M+Gly−H]$^-$, 493 (100) [M−H]$^-$, 476 (27) [M−H_2O]$^-$, 341 (20), 139 (16); Positive HR-ESIMS: found: 517.2576, calcd 517.2566 for $C_{30}H_{38}O_6Na$ [M+Na]$^+$.

3.3.7. Longipedlactone G (7). White powder; $[\alpha]_D^{25.2}$ −148.9 (*c* 0.62, C_5H_5N); UV (MeOH): λ_{max} (log ε)=271 (2.74), 225 nm (4.58); IR (KBr): ν_{max}=3520 (br), 2972, 2926, 2884, 2839, 1697, 1642, 1133 cm^{-1}; ^{1}H and ^{13}C NMR data, see Tables 2 and 3; Negative FABMS: *m/z* (%): 601 (3) [M+Gly−H]$^-$, 509 (100) [M−H]$^-$, 493 (23) [M−H_2O−H]$^-$, 339 (19), 325 (28), 297 (18), 167 (21), 138 (27), 123 (52); Negative HR-ESIMS: found: 509.2550, calcd 509.2539 for $C_{30}H_{37}O_7$ [M−H]$^-$.

3.3.8. Longipedlactone H (8). White powder; $[\alpha]_D^{23.3}$ −21.1 (*c* 0.85, C_5H_5N); UV (MeOH): λ_{max} (log ε)=278 (4.50), 202 nm (4.54); IR (KBr): *v*=3444 (br), 2927, 2855, 1697, 1130 cm^{-1}; ^{1}H and ^{13}C NMR data, see Tables 2 and 3; Negative FABMS: *m/z* (%): 603 (6) [M+Gly−H]$^-$, 511 (68) [M−H]$^-$, 494 (8) [M−H_2O]$^-$, 217 (7), 171 (10), 139 (100), 123 (14), 111 (10); Negative HR-ESIMS: found: 511.2695, calcd 511.2695 for $C_{30}H_{39}O_7$ [M−H]$^-$.

3.3.9. Longipedlactone I (9). White powder; $[\alpha]_D^{23.4}$ −30.5 (*c* 0.40, C_5H_5N); UV (MeOH): λ_{max} (log ε)=355 (2.57), 202 nm (4.66); IR (KBr): *v*=3445 (br), 2926, 2851, 1699, 1639, 1131 cm^{-1}; ^{1}H and ^{13}C NMR data, see Tables 2 and 3; Negative FABMS: *m/z* (%): 620 (29) [M+Gly−H]$^-$, 528 (80) [M]$^-$, 486 (55), 362 (22), 348 (83), 340 (100), 325 (31), 228 (24), 166 (12); Negative HR-ESIMS: found: 527.2622, calcd 527.2644 for $C_{30}H_{39}O_8$ [M−H]$^-$.

3.4. Cytotoxicity bioassays

Cytotoxicity of compounds against suspended tumor cells was determined by trypan blue exclusion method. Cytotoxicity against adherent cells was determined by sulforhodamine B (SRB) assay. Cells were plated in 96-well plate 24 h before treatment and continuously exposed to different concentrations of compounds for 72 h. After compound treatment, cells were counted (suspended cells) or fixed and stained with SRB (adherent cells) as described in Monks et al.[16]

3.5. X-ray crystallographic studies of 1 and 6

3.5.1. Longipedlactone A (1). $C_{30}H_{38}O_5\cdot CH_3OH$, *M*=510.63, orthorhombic system, space group $P2_12_12_1$, *a*=12.420 (3), *b*=14.407 (3), *c*=16.290 (3) Å, *V*=2914.9 (10) Å^3, *Z*=4, crystal dimensions 0.10×0.20×0.80 mm was used for measurements on a MAC DIP-2030K diffractometer with a graphite monochromator (ω scans, $2\theta_{max}$=50.0°), Mo Kα radiation. The total number of independent reflections measured was 3440, of which 2477 were observed ($|F|^2 \geq 2\sigma|F|^2$). Final indices: R_1=0.0751, wR_2=0.1150, *S*=0.494, $(\Delta/\sigma)_{max}$=0.005, $(\Delta/\rho)_{min}$=−0.463 e/Å^3, $(\Delta/\rho)_{max}$=0.433 e/Å^3.

3.5.2. Longipedlactone F (6). $C_{30}H_{38}O_6\cdot CH_3OH$, *M*=526.65, orthorhombic system, space group $P2_12_12_1$, *a*=12.275 (3), *b*=14.606 (3), *c*=16.360 (3) Å, *V*=2933.2 (10) Å^3, *Z*=4, crystal dimensions 0.50×0.50×0.50 mm was used for measurements on a MAC DIP-2030K diffractometer with a graphite monochromator (ω scans, $2\theta_{max}$=50.0°), Mo Kα radiation. The total number of independent reflections measured was 3609, of which 3606 were observed ($|F|^2 \geq 2\sigma|F|^2$). Final indices: R_1=0.0798, wR_2=0.1247, *S*=1.090, $(\Delta/\sigma)_{max}$=0.000, $(\Delta/\rho)_{min}$=−0.270 e/Å^3, $(\Delta/\rho)_{max}$=0.254 e/Å^3. The crystal structures (**1** and **6**) were solved by the direct method SHELX-86 (Sheldrich, G.M., University of Gottingen, Gottingen, Germany, 1985) and expanded using difference Fourier techniques, refined by the program and method NOMCSDP and the full-matrix least-squares calculations.[17] Crystallographic data for the structures of **1** and **6** have been deposited in the Cambridge Crystallographic Data Centre (deposition number: CCDC 292926 of **1**, and 292927 of **6**). Copies of these data can be obtained free of charge via www.ccdc.cam.ac.uk/conts/retrieving.html (or from the Cambridge Crystallographic Data Centre, 12, Union Road, Cambridge CB21EZ, UK; fax: +44 1223 336 033; or deposit@ccdc.cam.ac.uk).

Acknowledgements

This project was supported by grants from the National Natural Science Foundation of China (No. 20402016), the Natural Science Foundation of Yunnan Province (No. 2005XY04), and the Yong Academic and Technical

Leader Raising Foundation of Yunnan Province (No. 2005py01-32). The antitumor activity tests were carried out by the Tumor Research Laboratory, Shanghai Institute of Medicine Material, Chinese Academy of Sciences.

Supplementary data

Supplementary data associated with this article can be found in the online version, at doi:10.1016/j.tet.2006.03.108.

References and notes

1. Liu, J. S.; Li, L. *Phytochemistry* **1995**, *38*, 241–245.
2. Chen, D. F.; Zhang, S. X.; Mutsuo, K.; Sun, Q. Z.; Feng, J.; Wang, Q.; Teruo, M.; Yoshitaka, N.; Harukuni, T.; Hoyoku, N.; Wang, H. K.; Suan, L.; Morris, N.; Lee, K. H. *J. Nat. Prod.* **2002**, *65*, 1242–1245.
3. Chen, D. F.; Zhang, S. X.; Wang, H. K.; Zhang, S. Y.; Sun, Q. Z.; Cosentino, L. M.; Lee, K. H. *J. Nat. Prod.* **1999**, *62*, 94–97.
4. Yang, X. W.; Hirotsugu, M.; Masao, H.; Tsuneo, N.; Yasuhiro, T.; Tohru, K.; Chen, D. F.; Xu, G. J.; Toshihiko, H.; Michael, E.; Hiroshi, M. *Chem. Pharm. Bull.* **1992**, *40*, 1510–1516.
5. Li, S. Y.; Wu, M. D.; Wang, C. W.; Kuo, Y. K.; Huang, R. L.; Lee, K. H. *Chem. Pharm. Bull.* **2000**, *48*, 1992–1993.
6. Li, L. N.; Xue, H.; Tan, R. *Planta Med.* **1985**, *51*, 297–300.
7. Li, L. N.; Xue, H. *Planta Med.* **1986**, *52*, 492–493.
8. Liu, J. S.; Li, L. *Phytochemistry* **1993**, *33*, 1293–1296.
9. Shen, Y. C.; Lin, Y. C.; Chiang, M. Y.; Sheau, F. Y.; Cheng, Y. B.; Liao, C. C. *Org. Lett.* **2005**, *15*, 3307–3310.
10. Shen, Y. C.; Lin, Y. C.; Cheng, Y. B.; Kuo, Y. H.; Liaw, C. C. *Org. Lett.* **2005**, *23*, 5297–5300.
11. *Compilation of Chinese Herb Medicine*; People's Publishing House: Beijing, 1975; Vol. 1, p 581.
12. *Pharmacopoeia of the People's Republic of China*; People's Medical Publishing House: Beijing, 1977; Vol. 1, pp 396–397.
13. Pu, J. X.; Xiao, W. L.; Lu, Y.; Li, R. T.; Li, H. M.; Zhang, L.; Huang, S. X.; Li, X.; Zhao, Q. S.; Zheng, Q. T.; Sun, H. D. *Org. Lett.* **2005**, *22*, 5079–5082.
14. Tan, R.; Xue, H.; Li, L. N. *Planta Med.* **1991**, *57*, 87–88.
15. Luisa, U. R.; Carlos, M. C.; Ramon, G.; Concepcion, A.; Juan, D. H.; Pedro, J. N. *J. Nat. Prod.* **2002**, *65*, 1540–1546.
16. Monks, A.; Scudiero, D.; Skehan, P.; Shoemaker, R.; Paull, K.; Vistica, D.; Hose, C.; Langley, J.; Cronise, P.; Vaigro-Wolff, A. *J. Natl. Cancer Inst.* **1991**, *83*, 757–766.
17. Lu, Y.; Wu, B. M. *Chin. Chem. Lett.* **1992**, *3*, 637–640.